Improvement of Transient Response in Signal Transformation Approach by Proper Compensator Initialization

Ali Bazaei, S. O. Reza Moheimani, and Yuen K. Yong

***Abstract*— In this brief, the transient performance of the signal transformation approach (STA) is considerably enhanced by initializing the state vector of the compensator to appropriate values. For triangular reference tracking, it is shown that the proposed method is identical to the impulsive state multiplication (ISM) approach. Through simulations and experiments, we also show that the proposed method can be equally applied to improve the STA for arbitrarily shaped desired signals, where ISM is not applicable. Tracking efficacy of the proposed method compared with that of an ordinary feedback loop with a similar noise rejection performance is also demonstrated.**

***Index Terms*— Hybrid control system, impulsive state multiplication (ISM), signal transformation, triangular references.**

I. Introduction

TRACKING control with triangular references is a key enabling technology in raster scan devices such as scanning probe microscopes [1], optical scanners [2], selective laser sintering systems [3], and emerging probe-based data storage devices [4]. For a reasonable tracking performance with a triangular reference, an ordinary feedback control system needs a high closed-loop bandwidth because of the existence of high-frequency components in a triangle signal. However, plant uncertainties, actuation limitations, nonlinearities, unmodeled dynamics, and sensor noise usually limit the closed-loop bandwidth of the control system.

In applications such as nanopositioning [1], [4]–[6], where the effect of measurement noise on controlled variable should be restricted, it is very important to keep the closed-loop bandwidth low. However, reducing the closed-loop bandwidth can have an adverse effect on the tracking performance. This difficulty, which is a tradeoff between noise rejection and tracking performance, can be solved to some extent by employing methods such as iterative learning control [2] and command preshaping [7]. However, in the former, the number of iterations before convergence and the requisite computations are high, and in the latter, an accurate model of the plant is required, which may yield poor robustness against uncertainties.

In [8], the signal transformation approach (STA) for tracking of triangular references was proposed to tackle the aforementioned difficulty, i.e., to achieve a better tracking performance in a low-bandwidth feedback system. In this method, significant improvement in steady-state tracking performance is obtained compared with an ordinary feedback system with a similar closed-loop bandwidth [9], [10]. However, for a fast reference signal, the transient performance of the method may not be acceptable. A recent solution to this drawback is impulsive state multiplication (ISM) control, which is suitable for piecewise linear (affine) references such as triangular waveforms [11]–[14].

This brief introduces an alternative solution that leads to a better transient performance in STA. In the proposed method, named initialized signal transformation approach (ISTA), the initial states of the compensator are set to specific values based on the compensator and the reference parameters.

Manipulation of compensator states is also used by others to achieve better transient performances in feedback control systems. In reset control strategies, the transient performance is improved by changing compensator states at specific time instances when the tracking error crosses zero [15], [16]. However, reset control cannot handle time-varying exogenous signals [17]. In [18]–[22], the control performance of ordinary feedback systems was improved by manipulating the states of compensators at prespecified times and/or incorporating feedforward signals. However, in these methods, accurate knowledge of plant dynamics and complete or partial knowledge of plant states are required.

In this brief, it is also shown that the ISTA is exactly equivalent to ISM, if at least two integrators are included in the compensator. We also show that the proposed ISTA can equally improve the transient performance of a recently developed STA for reference signals with arbitrary shapes [23], where ISM is not applicable. Simulations and experiments are presented to investigate the robustness of the proposed method against disturbances and measurement noise. Capability of the method is also compared with an ordinary feedback system with similar noise rejection performance. In addition, closed-form relationships are obtained for SISO LTI systems having at least two poles at the origin and a high-frequency gain different from -1.

II. Conventional STA

A schematic view of the conventional STA for tracking of a triangular reference is shown in Fig. 1(a) [10]. The method incorporates signal transformation mappings Φ and Φ^{-1} in the ordinary feedback system shown in Fig. 1(b) to improve on the tracking performance. The mappings for a triangular reference with amplitude a_0 and period $2T$ are realized by piecewise constant gains and biases as follows:

$$g = (-1)^{\lfloor \frac{t}{T} \rfloor},\ b_2 = 2a_0 \left\lfloor \frac{t+T}{2T} \right\rfloor,\ b_1 = -gb_2 \tag{1}$$

Manuscript received September 6, 2012; accepted April 19, 2013. Manuscript received in final form May 3, 2013. Date of publication June 7, 2013; date of current version February 14, 2014. This work was supported by the Australian Research Council. Recommended by Associate Editor G. Cherubini.

The authors are with the School of Electrical and Computer Engineering, University of Newcastle Australia, Callaghan NSW 2308, Australia (e-mail: ali.bazaei@newcastle.edu.au; reza.moheimani@newcastle.edu.au; yuenkuan.yong@newcastle.edu.au).

Color versions of one or more of the figures in this paper are available online at http://ieeexplore.ieee.org.

Digital Object Identifier 10.1109/TCST.2013.2261875

where $\lfloor . \rfloor$ is the floor function. Mappings Φ and Φ^{-1} are specifically designed to transform a triangular input into a ramp output and vice versa, respectively. To elucidate how this method improves the steady-state performance, assume the plant is stable, has a unity dc gain, and a sufficiently high bandwidth so that the ideal plant input for exact tracking of the triangular reference is equal to itself plus a square wave signal, as shown in Fig. 1(a). The compensator includes at least two integrators (two poles at the origin) so that it can generate a biased ramp signal after receiving a transient error signal e, which can be transformed into the ideal plant input by mapping Φ^{-1}. Thus, when plant output x in Fig. 1(a) closely follows the triangular reference in steady state, signals v and y at the input and output of mappings Φ^{-1} and Φ follow ramp signals, which are much smoother than the ideal plant input and the triangular reference. Therefore, the compensator has to attenuate a much smoother error signal e in Fig. 1(a) rather than a tracking error with sharp points in the ordinary feedback system of Fig. 1(b) (the plant output is usually smooth because of the integration and the zero feedthrough term in its state-space dynamics). In other words, because of the transformation mappings, the compensator in STA system attenuates the error because of the ramp reference signal r, which is much easier to follow compared with a triangular one. In addition, the requirement to track smoother references allows design of loops with lower bandwidth that merit more attenuation of measurement noise without sacrificing the steady-state tracking performance. Using internal model principle [24], at least two poles at the origin are required in the compensator to accurately track a ramp reference signal. If the plant dynamics can be approximated by a pair of stable complex poles and no zeros, a second-order strictly proper compensator with poles at the origin can be readily designed to achieve a stable loop with gain and phase margins greater than 10 dB and 10°, respectively (see [10, Sec. 5.2]).

As shown in [10], steady-state tracking performance of a triangular reference in the ordinary control system shown in Fig. 1(b) considerably improved when the signal transformation mappings Φ and Φ^{-1} are incorporated in the loop, as shown in Fig. 1(a), and the following conditions are met.

1) The open-loop plant dynamics can be approximated by a stable transfer function whose dc gain is equal to 1, and the magnitudes of the dominant zeros are sufficiently larger than those of the dominant poles.
2) To provide zero steady-state error for tracking of a ramp reference, at least two integrators (two poles at $s = 0$) are incorporated into the compensator.
3) If the signal transformation mappings are reduced to identity functions, the resulting system, shown in Fig. 1(b), is stable, and its phase and gain margins exceed 10° and 10 dB, respectively [10].
4) The open-loop bandwidth of the plant is sufficiently larger than that of the ordinary closed-loop system in Fig. 1(b) to represent a two-time-scale system, where the fast modes correspond to the plant and the slow modes belong to the compensator. In other words, if the plant is replaced by a unity gain (an infinitely fast stable dynamics) in Fig. 1(b), the resulting system remains stable and approximates the slow dynamics of the two-time-scale system. More details on this condition were presented in [23], where a zero feedthrough term was used for the compensator.
5) The triangular reference signal has a sufficiently large fundamental period so that stability condition $\gamma = \left|\lambda_{\max}\left(\widehat{A}\right)\right| < 1$ is satisfied.

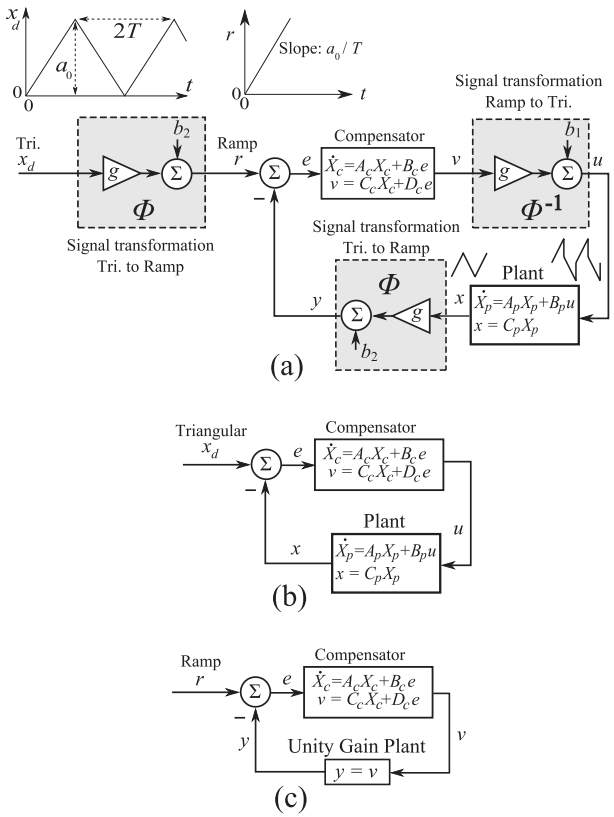

Fig. 1. (a) Details of STA and ISTA systems designed for the depicted triangular reference. The sharp points of the original reference are transformed into a smooth ramp reference, which is easier to follow. (b) Ordinary control system when mappings Φ and Φ^{-1} are replaced by identity functions. Because of the inherent smoothness of the plant output, the sharp slope discontinuities of the reference are transmitted into the error signal, aggravating the tracking performance. (c) Slow subsystem that estimates the compensator dynamics in the closed-loop STA system as shown in Fig. 1(a).

In condition 5, $\lambda_{\max}$ refers to the eigenvalue with the maximum magnitude, $\widehat{A}$ is $E\widehat{I}$, where $E = e^{AT}$ and $\widehat{I} = \left[-I_{n_p}, 0; 0, I_{n_c}\right]$. I_{n_p} and I_{n_c} are identity matrices, whose dimensions are n_p and n_c and correspond to those of the plant and compensator, respectively. Matrix A is defined as $\left[A_p - B_p D_c C_p, B_p C_c; -B_c C_p, A_c\right]$, which is the closed-loop state matrix of the system in Fig. 1(b). Here, the compensator can assume a nonzero feedthrough term D_c, which was zero in [10], however, results of Theorem 2 in reference [10] are still valid for $D_c \neq 0$ when B and A are the input and state matrices of the closed-loop system in Fig. 1(a), i.e., $B = \left[B_p D_c; B_c\right]$ and A as defined earlier. However, if the ordinary system in Fig. 1(b) has a very low closed-loop bandwidth or poor stability margins, and/or the frequency of the triangular reference is too high such that γ is very close to unity, conventional STA cannot provide an

acceptable transient performance [8], [10]. In the next section, we propose a solution to the foregoing shortcoming in STA.

III. Improving the Transient Performance

The strategy opted here to enhance the transient performance in STA is to set the initial states of the compensator to suitable values rather than the zero initial states in the conventional STA. Through the two-time-scale properties mentioned in Section II (Condition 4), we can approximate the transient behavior of the system by replacing the plant with a unity gain constant. In other words, the transient performance is dominated by the slow modes of the compensator rather than the plant fast modes. After the replacement, the direct series combination of mappings Φ^{-1} and Φ cancels their actions and the system is reduced to the slow subsystem shown in Fig. 1(c), which approximates the transient response of the STA system. Therefore, any action that improves the transient performance in the slow subsystem can similarly benefit the original system. In such estimation of the transient, only knowledge of stability and low-frequency gain of the plant are used. As the plant dynamics are not present in the approximate system in Fig. 1(c), the proposed method for transient response improvement will have inherent robustness to the initial states and bandwidth of the plant. Hence, if there exist specific values for initial states of the compensator to improve the transient performance of the slow subsystem, they will be good candidates for introducing a similar improvement in the STA system. The aforementioned first-order assumption about the plant, which was made for simplicity, will be relaxed subsequently. In the following theorem, we formulate the initial conditions of the compensator so that the transient component in the slow subsystem is reduced to zero and the steady-state response starts from the beginning.

Theorem 1: If $D_c \neq -1$ and the initial states of the compensator in Fig. 1(c) are selected as follows:

$$X_c(0) = -\frac{\left(A_c - \frac{B_c C_c}{1+D_c}\right)^{-2} B_c a_0}{T(1+D_c)} \tag{2}$$

then the response of the slow subsystem to the ramp reference $r = a_0 t/T$ will be free from any transient component.

Proof: The state-space representation of the closed-loop slow subsystem in Fig. 1(c) has state and input matrices as $A_{cl} = A_c - B_c C_c/1 + D_c$ and $B_{cl} = B_c/1 + D_c$, respectively. Thus, the closed-loop state response of the system can be written as follows:

$$X_c(s) = (sI - A_{cl})^{-1}\left[X_c(0) + \frac{B_c a_0}{T(1+D_c)s^2}\right]. \tag{3}$$

Using partial fraction expansion methods, the right-hand side of (3) can be partitioned into transient and steady-state components as follows:

$$(sI - A_{cl})^{-1} V(s) + \frac{V_1}{s} + \frac{V_2}{s^2} \tag{4}$$

where $V_1 = -A_{cl}^{-2} B_c a_0/T(1+D_c)$ and $V_2 = -A_{cl}^{-1} B_c a_0/T(1+D_c)$ are vectors with constant elements. Using the equality of the right-hand side of (3) with (4), the elements of vector $V(s)$ in (4) are also constants and do not depend on s. Therefore, the system in Fig. 1(c) has a total response that can be expressed in the following form:

$$X_c(s) = \overbrace{(sI - A_{cl})^{-1}\left[X_c(0) + \frac{A_{cl}^{-2} B_c a_0}{T(1+D_c)}\right]}^{\text{Transient}} \underbrace{-\frac{(sI + A_{cl}) A_{cl}^{-2} B_c a_0}{T(1+D_c)s^2}}_{\text{Steady state}}. \tag{5}$$

If we set the compensator's initial state equal to $X_c(0)$ in (2), the transient part of the overall response in the slow subsystem is reduced to zero and the closed-loop response of the slow subsystem starts from its steady-state value at the beginning. ■

Thus, the initial state vector in (2) is proposed for the compensator in Fig. 1(a) to improve the transient performance of the STA system. In the next section, we demonstrate how the suggested method, which is called ISTA, can considerably improve the performance of conventional STA.

A. Simulation Results

In this example, we assume that the plant has the following transfer function:

$$P(s) = \frac{\left(1 + \frac{s}{7000}\right)}{\left(1 + \frac{s}{5000}\right)^2 \left(1 + \frac{s}{10000}\right)}. \tag{6}$$

The compensator's state-space representation, which has two poles at the origin, is described by the following matrices:

$$\begin{aligned} A_c &= \begin{bmatrix} -40 & 0 & 0 \\ 8 & 0 & 0 \\ 0 & 2 & 0 \end{bmatrix} \\ B_c &= \begin{bmatrix} 64 \\ 0 \\ 0 \end{bmatrix} \\ D_c &= 0 \\ C_c &= \begin{bmatrix} 0.78125 \\ 39.453125 \\ 78.125 \end{bmatrix}^{\mathrm{T}}. \end{aligned} \tag{7}$$

Compared with 560-Hz bandwidth of the plant, the closed-loop bandwidth of the system is just 35 Hz, which is consistent with the fourth condition in Section II and results in significant attenuation of measurement noise. The fundamental frequency of the triangular reference is 100 Hz and its amplitude is 1 ($a_0 = 1$). From (2), the compensator's states should be initialized as $X_c(0) = [0 \ 1.28 \ -0.6464]^{\mathrm{T}}$. With zero initial conditions for the plant, the transient performance of the tracking errors with the states of the compensator in Fig. 1(a) initialized to the proposed values are indicated by ISTA in Fig. 2. If the compensator starts from zero initial conditions, which is the conventional STA, the response shown by the STA label in Fig. 2 is obtained. Clearly, the proper selection of compensator initial conditions can significantly improve the transient performance of STA without altering the steady-state response.

Remark 1: The STA system in Fig. 1(a) is sensitive to variation of plant dc gain and constant disturbances [25]. However, using suitable inner feedback loops on the original plant and applying the STA system in the outer loop, which is demonstrated in Section V, we can provide acceptable robustness against plant uncertainties and disturbances in STA [10, Sec. IV], [23, Sec. X], [25, Sec. V]. Considering that the initial conditions of the compensator have generally no effect on the system robustness, the foregoing robustifying schemes are readily applicable in ISTA.

IV. Connection With ISM

In [11]–[14], the method known as ISM was introduced to track a triangular reference with improved transient performance compared with the conventional STA. ISM is a simplified version of STA for triangular references, in which the reference is also fed as a feedforward term and the input and output of the compensator are multiplied by square wave signals, as shown in Fig. 3(c). Although the connection between ISM and the conventional STA was studied for triangular references and zero initial conditions in [12] and [14], the effect of nonzero initial conditions in the compensator was not addressed. In addition, in contrast to ISM, which only deals with affine references, ISTA and STA are also applicable to a more general class of references (Section V and [23]). The following theorem reveals the connection between ISTA and ISM for triangular references.

Theorem 2: The STA system in Fig. 1(a) for tracking of triangular references is equivalent to the ISM method if the compensator has at least two poles at the origin and its initial conditions (in the STA system) are set according to (2).

Proof: Consider the ISTA, which corresponds to Fig. 1(a) with the compensator initialized according to (2). We can move the two identical signal transformation blocks Φ forward passed the left sum block and merge them into a gain $g(t)$ behind the compensator, as shown in Fig. 3(a). If a ramp signal $r(t) = a_0 t/T$ is applied to mapping Φ^{-1}, its output will be the triangular reference x_d. Thus, $b_1(t)$ can be written as follows:

$$b_1(t) = x_d(t) - g(t)r(t). \tag{8}$$

Hence, we can represent the ISTA system as shown in Fig. 3(a). The initialized LTI compensator is equivalent to its duplicate with zero initial conditions, while its output is added by the response of compensator output just because of its initial conditions (zero-input response), as shown in Fig. 3(b). The zero-input response is exactly equal to the ramp reference.[1] Thus, the ISTA system in Fig. 1(a) is exactly equal to the system in Fig. 3(c). According to Section II, $g(t)$ is a square wave signal that switches between $+1$ and -1. Using Theorem 3 in [12], if we introduce $i = \lfloor t/T \rfloor$, $t_i := iT$, and $q_i := g^{-1}(t_i) = (-1)^i$, we deduce that the system within the dotted rectangle in Fig. 3(c) is an ISM system representing the dynamics from $w(t)$ to $z(t)$ as follows:

$$\left.\begin{aligned} &\dot{X}(t) = A_c X(t) + B_c w(t), \ \text{if: } t \neq t_i, \\ &X(t_i) = \tfrac{q_i}{q_{i-1}} X(t_i^-) = -X(t_i^-), \\ &z(t) = C_c X(t) \end{aligned}\right\} \tag{9}$$

where $i = 1, 2, 3, \cdots$. Therefore, when the compensator keeps at least two integrators, the ISTA will be exactly equal to the ISM method, even during the transient. ■

[1]According to Theorem 1, if the system in Fig. 1(c) starts with initial condition (2), the output will exactly follow the ramp reference from scratch. Thus, the compensator's input signal e is identically zero, as if the loop is left open and the compensator is just driven by its initial condition. Therefore, the open-loop response of the compensator to the initial condition (2) is exactly equal to the ramp reference.

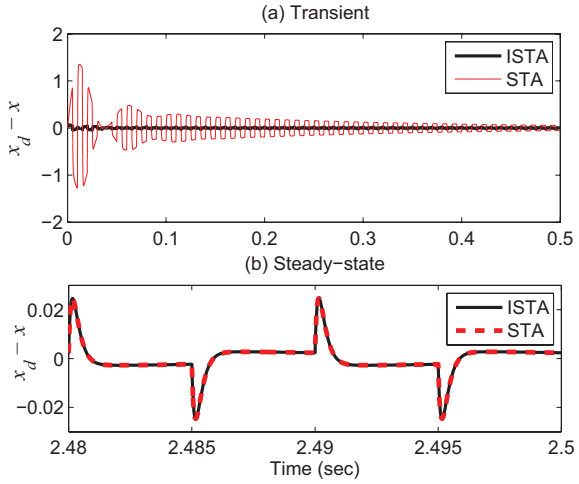

Fig. 2. Response of the tracking errors in STA and ISTA systems with 35-Hz closed-loop bandwidth, designed to track a triangular signal with unity amplitude and 100-Hz fundamental frequency.

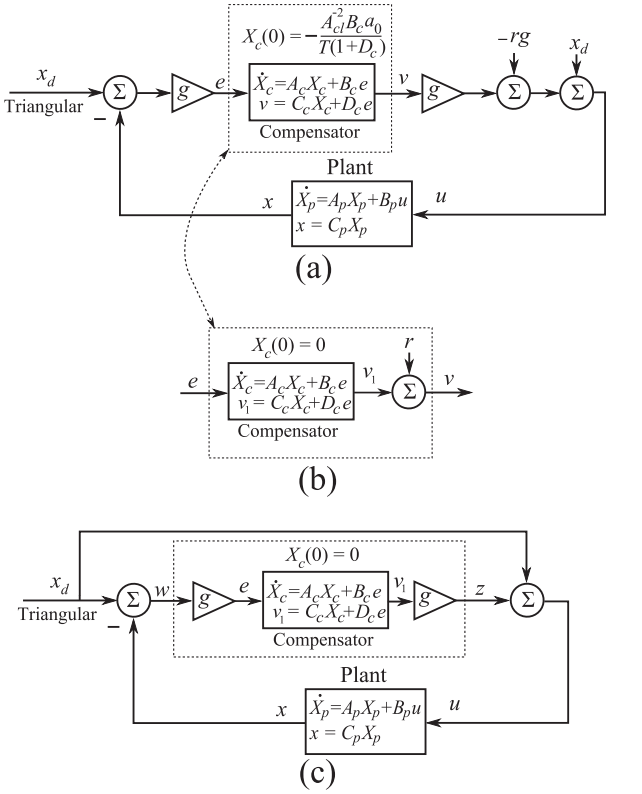

Fig. 3. (a) Reduction of two mappings Φ in Fig. 1(a) into gain $g(t)$ and decomposition of mapping Φ^{-1}. (b) Equivalent of the LTI compensator with nonzero initial conditions. (c) Equivalent of ISTA system for triangular reference, which is also the ISM method.

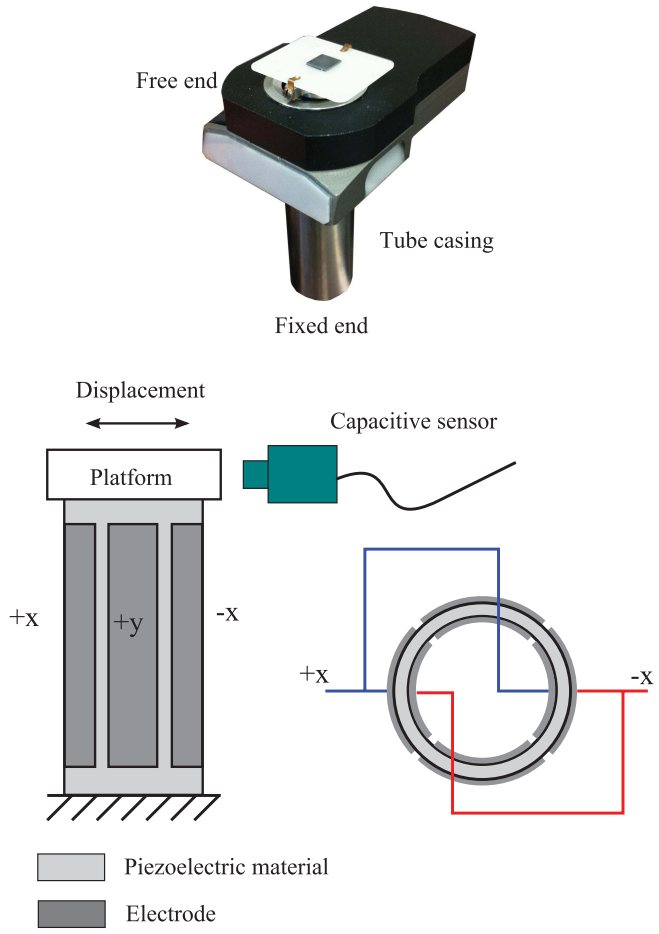

Fig. 4. Demonstration of the piezoelectric tube scanner and schematics of its four-quadrant electrode pads driven by opposite voltages to create a push–pull actuation along the x-axis. The deflection at the free end of the tube is measured by a displacement capacitive sensor.

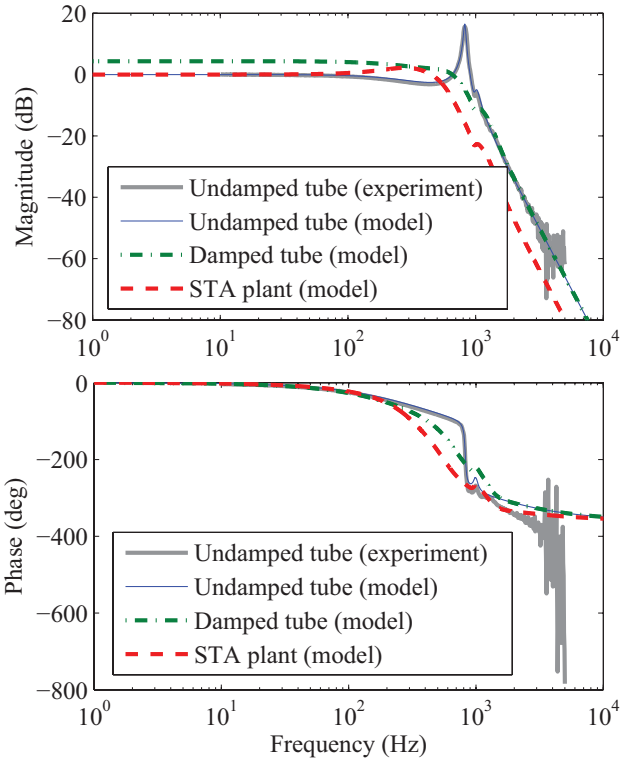

Fig. 5. Bode diagrams for the open-loop plant [LTI model (11) of the undamped tube plotted by a thin blue line and the experimental data by the thick gray line]; the damping loop (dashed-dotted green line); and the robustification loop or STA plant (dashed red line).

V. ISTA for Nonaffine Reference Signals

In addition to triangular references, the STA method can also be developed to handle arbitrarily shaped reference signals [23]. In this section, we demonstrate how a proper initialization of compensator can considerably improve the transient performance of STA system for a nonaffine reference. Apart from the reference signal shape, the STA system is similar to Fig. 1(a), where the signal transformation blocks Φ and Φ^{-1} are designed such that they can perform conversions between the reference signal and a ramp reference $r = a_0 t$. As the reference profile $x_d(t)$ is not constrained to be triangular, the required signal transformation operators can be more sophisticated than those mentioned in Section II. Assuming similar circumstances as stated in Section II, we can show that the compensator dynamics in the STA system can be approximated by the slow subsystem in Fig. 1(c). Substituting the slope a_0/T of the ramp reference by a_0 in Theorem 1, we can improve the transient performance using the following initial conditions for the compensator

$$X_c(0) = -\frac{A_{cl}^{-2} B_c a_0}{1 + D_c}. \tag{10}$$

To illustrate this approach experimentally, the x-axis of a commercial piezoelectric tube scanner in an AFM nanopositioner is used as the plant, which is a piezoelectric material with four-quadrant electrodes shown in Fig. 4 [26]. The device has the experimental bode plots shown in Fig. 5 with a large resonance peak, which is not generally suitable for accurate tracking of fast reference signals. We procured the following LTI model for the undamped plant, which reasonably fits the experimentally collected data as shown in Fig. 5

$$\frac{1 + \frac{s}{61575} + \left(\frac{s}{6157.5}\right)^2}{1 + \frac{s}{1515} + \left(\frac{s}{2737}\right)^2 + \left(\frac{s}{2883}\right)^3 + \left(\frac{s}{3774}\right)^4 + \left(\frac{s}{4361}\right)^5 + \left(\frac{s}{5174}\right)^6}. \tag{11}$$

To ameliorate the undesirable resonant behavior of the plant, we use the feedback control structure surrounded by the dashed line in Fig. 6, which functions as a damping loop. Using the conventional method described in [25], we obtain the following damping controller:

$$C_{\mathrm{PPF}}(s) = 0.4 \frac{\frac{s}{1821} + 1}{\frac{s^2}{8000^2} + \frac{2 \times 0.34 s}{8000} + 1}. \tag{12}$$

The damping loop has stability margins of 8 dB and -49° and its bode and step responses are also included in Fig. 5, demonstrating an effective damping of the resonance. The controller $C_{\mathrm{PPF}}(s)$ has a positive low-frequency gain, which accords with positive position feedback (PPF). PPF is a damping method used in many structurally flexible systems [27]. Using negative imaginary theory, the stability of

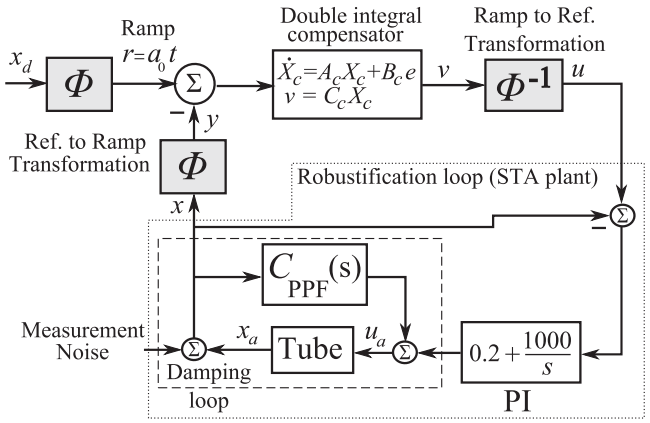

Fig. 6. Details of the STA and ISTA systems used for the tube scanner.

PPF control systems are readily guaranteed subject to simple criteria [28]. A requirement for STA system in Fig. 1(b) is that the plant should have a low-frequency gain equal to one. The damped tube does not have a unity low-frequency gain. In addition, it may change gradually because of unwanted drift in the dc gain of the tube. This difficulty can be resolved by wrapping a PI loop around the damping loop, which is indicated by the dotted line in Fig. 6. The integrator in the PI loop guarantees an exact unity dc gain for the plant block (STA plant) regardless of the fluctuations in the tube dc gain. The gain and phase margins of the PI loop are 7 dB and 47°, respectively, and its bandwidth is about 548 Hz. The bode and step responses of the PI loop are indicated by STA plant in Fig. 5. Fig. 6 shows the complete schematic of the STA controller. We opt the following reference signal, as an arbitrary nonaffine waveform with period T_1+T_2:

$$x_d(t)=\begin{cases} f_1(t)=\alpha \sin h\left(\frac{t-\frac{T_1}{2}}{\beta_1}\right),\ t\in[0,T_1), \\ f_2(t)=-\alpha \sin h\left(\frac{t-T_1-\frac{T_2}{2}}{\beta_2}\right),\ t\in[T_1,T_1+T_2) \end{cases} \tag{13}$$

where $\alpha=a_0/107.393$, $\beta_l=T_l/10.7393$, $l\in\{1,2\}$, and a_0 is the reference amplitude. Contrary to repetitive controllers [29], repetition is not necessary in STA and ISTA systems, as shown by the example in [23], where the reference period is long and the steady state almost starts before the end of the first period. Compared with the slope of a triangular waveform having similar amplitude and period, the slope of the selected reference changes considerably (from 0.05 to 5.37 times the triangle's slope). Thus, tracking control with the selected reference is very difficult compared with the foregoing triangular reference. Selecting the profile of the reference and using the synthesis scheme as reported in [23], mappings Φ and Φ^{-1} in Fig. 6 are obtained as follows:

$$y=\begin{cases} a_0\left[\Delta(t)+\frac{T_1}{2}+\beta_1 \text{arcsin}h\left(\frac{x}{\alpha}\right)\right],\ \text{if: } S=1 \\ a_0\left[\Delta(t)+T_1+\frac{T_2}{2}-\beta_2 \text{arcsin}h\left(\frac{x}{\alpha}\right)\right],\ \text{if: } S=2 \end{cases} \tag{14}$$

and

$$u=f_k\left(\frac{v}{a_0}-\Delta(t)\right),\ \text{if: } S(t)=k \tag{15}$$

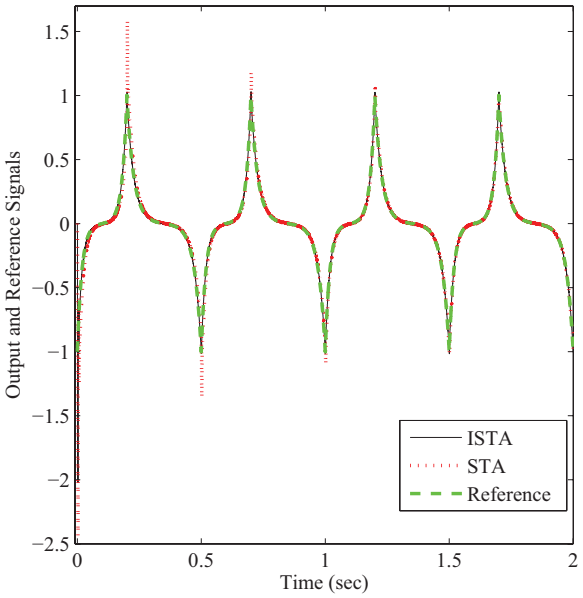

Fig. 7. Profiles of the tube output and the reference signal in the experimentally implemented ISTA and STA systems.

where $\Delta(t)=T\lfloor t/T\rfloor$, and

$$S(t)=\begin{cases} 1,\ \text{if: } t-\Delta(t)<T_1 \\ 2,\ \text{if: otherwise} \end{cases}. \tag{16}$$

The compensator dynamics in the STA system has two poles at the origin, which are described as follows:

$$\begin{aligned} A_c&=\begin{bmatrix}0&1\\0&0\end{bmatrix} \\ B_c&=\begin{bmatrix}0\\1\end{bmatrix} \\ C_c&=\begin{bmatrix}180\\120\end{bmatrix}^T \\ D_c&=0. \end{aligned} \tag{17}$$

The corresponding ordinary feedback system in Fig. 1(b), which is obtained if we substitute the mappings in Fig. 6 by identity functions, has a bandwidth of 21 Hz and gain and phase margins of 21.5 dB and 85°, respectively. Using $a_0=1$, and (17) and (10), the proposed initial state for the compensator is $[-0.00\overline{37}, 0.00\overline{5}]^T$. Selecting $T_1=0.2$ s and $T_2=0.3$ s, the resulting reference signal is shown in Fig. 7 with the thick dashed line. After implementing the STA with the proposed initialization (ISTA), the controlled plant output is also shown in Fig. 7 with a solid line. Also, included in Fig. 7, are the plant output controlled by implementing STA method with zero initial conditions (STA). Fig. 8 shows the corresponding tracking errors. Clearly, the transient performance of STA is remarkably improved by the proposed initialization of the compensator. In addition, the steady-state tracking performance is not compromised. The profiles of manipulated inputs, shown in Fig. 9(c), show that both ISTA and STA have acceptable actuations for the nonaffine reference. The noticeable differences among these profiles result from the inherent nonlinearities of the piezoelectric tube, such as hysteresis and creep. The excellent control performance of

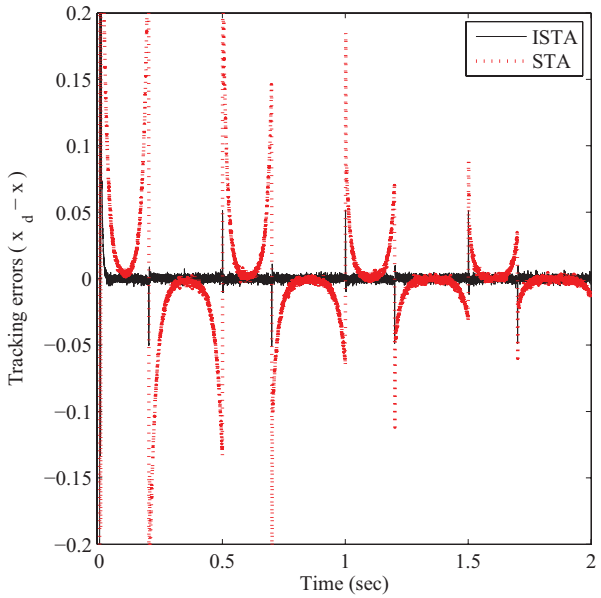

Fig. 8. Profiles of the tracking errors in ISTA and STA systems.

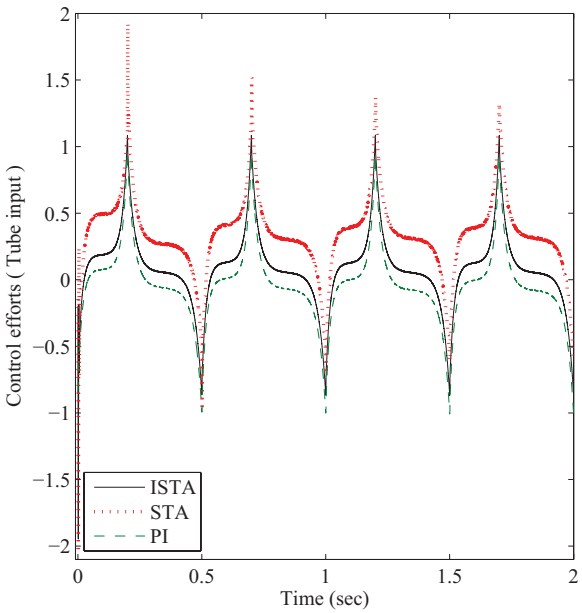

Fig. 9. Manipulated inputs applied to the tube in ISTA and STA systems, and also the ordinary PI control system.

the ISTA system in the presence unmodeled tube nonlinearities reveals the high robustness of the proposed method.

As ISTA is a hybrid control method, it is also important to compare its tracking performance with that of an ordinary feedback system with similar noise rejection performance. As the ordinary system, we use the PI control system, surrounded by the dotted polygon in Fig. 6. We multiply the PI gains in the ordinary system by 1.08. Thus, the ordinary system has a similar noise rejection performance as that of the foregoing ISTA scheme. The noise rejection performance is measured as the percentage of reduction in the root mean square (rms) value of the noise source, when transmitted into the actual plant output through the closed-loop system. This performance is evaluated using the plant model for simulation of control system. For the ISTA system in Fig. 6, the noise rejection performance is the rms value of the real tube output x_a divided

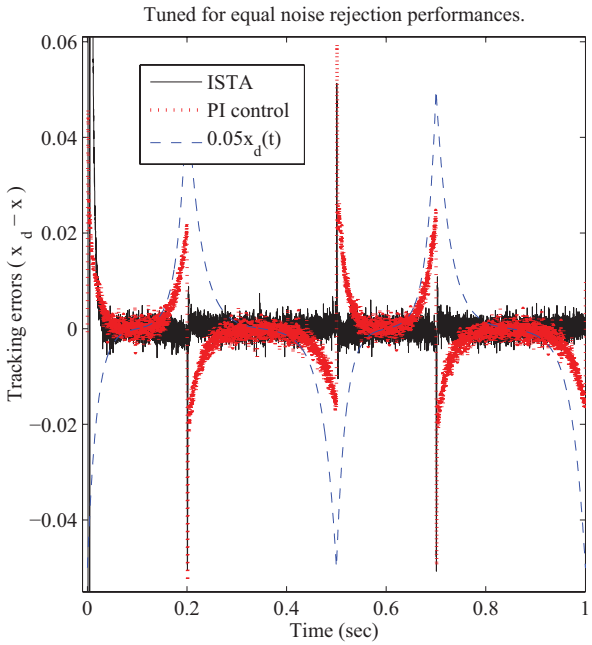

Fig. 10. Comparison of tracking error in ISTA with that of an ordinary PI control method with the nonaffine reference and same noise rejection capability.

by that of a zero-mean noise source, when Φ and Φ^{-1} are substituted by unity gains and the other exogenous inputs are reduced to zero. This method of noise performance evaluation for STA system was validated in [23]. The noise rejection performance for the ordinary system is defined accordingly. Time histories of the tracking errors along with the scaled reference signal, shown in Fig. 10, reveal that the proposed hybrid system considerably improves the control performance compared with the ordinary feedback system.

VI. Conclusion

Appropriate values were derived for initial values of the compensator states, which can considerably improve the transient performance of STA without adverse effects on the steady-state performance. As the initial values only depend on compensator and reference parameters, the robust performance of the method was preserved as well. When the compensator had at least two integrators and the reference was triangular, it showed that the proposed ISTA was equivalent to the ISM method, which was a recently proposed method for tracking of piecewise linear references. ISTA can also be applied to improve the transient in STA method for arbitrarily shaped reference signals, where ISM is not applicable. Efficacy and applicability of the proposed method were confirmed by experimentally implementing ISTA, STA, and a traditional controller.

References

[1] S. Devasia, E. Eleftheriou, and S. O. R. Moheimani, "A survey of control issues in nanopositioning," *IEEE Trans. Control Syst. Technol.*, vol. 15, no. 5, pp. 802–823, Sep. 2007.

[2] J. Yen, Y. Yeh, Y. Peng, and J. Lee, "Application of the continuous no-reset switching iterative learning control on a novel optical scanning system," *Mechatronics*, vol. 19, no. 1, pp. 65–75, 2009.

[3] D. Zhiqiang, Z. Zude, A. Wu, and C. Youping, "A linear drive system for the dynamic focus module of SLS machines," *Int. J. Adv. Manuf. Technol.*, vol. 32, nos. 11–12, pp. 1211–1217, 2007.

[4] A. Pantazi, A. Sebastian, T. A. Antonakopoulos, P. Bächtold, A. R. Bonaccio, J. Bonan, G. Cherubini, M. Despont, R. A. DiPietro, U. Drechsler, U. Dürig, B. Gotsmann, W. Häberle, C. Hagleitner, J. L. Hedrick, D. Jubin, A. Knoll, M. A. Lantz, J. Pentarakis, H. Pozidis, R. C. Pratt, H. Rothuizen, R. Stutz, M. Varsamou, D. Wiesmann, and E. Eleftheriou, "Probe-based ultrahigh-density storage technology," *IBM J. Res. Develop.*, vol. 52, no. 4, pp. 493–511, 2008.

[5] Y. K. Yong, K. Liu, and S. O. R. Moheimani, "Reducing cross-coupling in a compliant XY nanopositioning stage for fast and accurate raster scanning," *IEEE Trans. Control Syst. Technol.*, vol. 18, no. 5, pp. 1172–1179, Sep. 2010.

[6] A. Pantazi, A. Sebastian, G. Cherubini, M. Lantz, H. Pozidis, H. Rothuizen, and E. Eleftheriou, "Control of MEMS-based scanning-probe data-storage devices," *IEEE Trans. Control Syst. Technol.*, vol. 15, no. 5, pp. 824–841, May 2007.

[7] H. Suzuki and T. Sugie, "Off-line reference shaping of periodic trajectories for constrained systems with uncertainties," *IEEE Trans. Autom. Control*, vol. 53, no. 6, pp. 1531–1535, Jul. 2008.

[8] A. Sebastian and S. O. R. Moheimani, "Signal transformation approach to fast nanopositioning," *Rev. Sci. Instrum.*, vol. 80, pp. 076101-1–076101-3, Jul. 2009.

[9] A. Bazaei, Y. K. Yong, S. O. R. Moheimani, and A. Sebastian, "Tracking control of a novel AFM scanner using signal transformation method," in *Proc. 5th IFAC Symp. Mech. Syst.*, Cambridge, MA, USA, Sep. 2010, pp. 84–89.

[10] A. Bazaei, S. O. R. Moheimani, and A. Sebastian, "An analysis of signal transformation approach to triangular waveform tracking," *Automatica*, vol. 47, pp. 838–847, Apr. 2011.

[11] T. Tuma, A. Pantazi, J. Lygeros, and A. Sebastian, "Tracking of high frequency piecewise affine signals using impulsive control," in *Proc. 5th IFAC Symp. Mech. Syst.*, 2010, pp. 90–95.

[12] T. Tuma, A. Pantazi, J. Lygeros, and A. Sebastian, "Impulsive control for nanopositioning: Stability and performance," in *Proc. 14th Int. Conf. Hybrid Syst., Comput. Control*, 2011, pp. 173–180.

[13] T. Tuma, A. Sebastian, W. Haberle, J. Lygeros, and A. Pantazi, "Impulsive control for fast nanopositioning," *Nanotechnology*, vol. 22, no. 13, pp. 135501-1–135501-6, 2011.

[14] T. Tuma, A. Pantazi, J. Lygeros, and A. Sebastian, "Comparison of two nonlinear control approaches to fast nanopositioning: Impulsive control and signal transformation," *Mechatronics*, vol. 22, no. 3, pp. 302–309, 2012.

[15] J. Clegg, "A nonlinear integrator for servomechanism," *Trans. Amer. Inst. Electr. Eng. II, Appl. Ind.*, vol. 77, no. 1, pp. 41–42, 1958.

[16] Y. Chait and C. Hollot, "On Horowitz's contributions to reset control," *Int. J. Robust Nonlinear Control*, vol. 12, no. 4, pp. 335–355, 2002.

[17] O. Beker, C. Hollot, and Y. Chait, "Forced oscillations in reset control systems," in *Proc. 39th IEEE Conf. Decision Control*, vol. 5. Sydney, NSW, Australia, Dec. 2000, pp. 4825–4826.

[18] M. Johansson, "Optimal initial value compensation for fast settling times in mode-switching control systems," in *Proc. 39th IEEE Conf. Decision Control*, vol. 5. Sydney, NSW, Australia, Dec. 2000, pp. 5137–5142.

[19] T. Izumi, A. Kojima, and S. Ishijima, "Improving transient with compensation law," in *Proc. 15th IFAC World Congr.*, Barcelona, Spain, 2002, p. 109.

[20] T. Doh and J. Ryoo, "A linear matrix inequality approach to initial value compensation for mode switching control in hard disk drive servo systems," in *Proc. Int. Conf. Control, Autom. Syst.*, Seoul, Korea, Oct. 2008, pp. 1692–1695.

[21] N. Hara and K. Konishi, "Compensation law for constrained systems with initial state uncertainty based on piecewise affine function," in *Proc. 18th Medit. Conf. Control Autom.*, Jun. 2010, pp. 389–394.

[22] Y. Guo, Y. Wang, L. Xie, H. Li, and W. Gui, "Optimal reset law design and its application to transient response improvement of HDD systems," *IEEE Trans. Control Syst. Technol.*, vol. 19, no. 5, pp. 1160–1167, Sep. 2011.

[23] A. Bazaei and S. Moheimani, "Signal transformation approach to tracking control for arbitrary references," *IEEE Trans. Autom. Control*, vol. 57, no. 9, pp. 2294–2307, Sep. 2012.

[24] B. Francis and W. Wonham, "The internal model principle of control theory," *Automatica*, vol. 12, no. 5, pp. 457–465, 1973.

[25] A. Bazaei, Y. K. Yong, S. O. R. Moheimani, and A. Sebastian, "Tracking of triangular references using signal transformation for control of a novel AFM scanner stage," *IEEE Trans. Control Syst. Technol.*, vol. 20, no. 2, pp. 453–464, Mar. 2012.

[26] S. O. R. Moheimani, "Invited review article: Accurate and fast nanopositioning with piezoelectric tube scanners: Emerging trends and future challenges," *Rev. Sci. Instrum.*, vol. 79, no. 7, pp. 071101-1–071101-11, Jul. 2008.

[27] G. Song and B. Agrawal, "Vibration suppression of flexible spacecraft during attitude control," *Acta Astron.*, vol. 49, no. 2, pp. 73–83, 2001.

[28] I. R. Petersen, "Negative imaginary systems theory in the robust control of highly resonant flexible structures," in *Proc. Austral. Control Conf.*, Melbourne, Australia, Nov. 2011, pp. 1–6.

[29] Q. Quan and K. Cai, "A survey of repetitive control for nonlinear systems," *Sci. Found. China*, vol. 18, no. 2, pp. 45–53, 2010.